EasyChair Preprint

№ 10341

Advances in Thermal Barrier Coatings (TBC) for High Temperature Gas Turbines

Zahid Mehmood, Ali Sarosh and Osama Ali Ahmed Awan

June 6, 2023

Recent Advancements in Thermal Barrier Coatings (TBC) for High-Temperature Gas Turbines

Zahid Mehmood[a]
De22partment of Aerospace Engineering
CAE, NUST
H-9 Islamabad, Pakistan
Zahid_mehmood@cae.nust.edu.pk

Prof. Dr. Ali Sarosh[b,*]
Department of Mechanical and Aerospace engineering
Air University
E-9 Islamabad, Pakistan
ali.sarosh@mail.au.edu.pk

Osama Ali Ahmed Awan[c]
Department of Mechanical and Aerospace engineering
Air University
E-9 Islamabad, Pakistan
osamaaliahmadwan@outlook.com

Abstract*— Gas turbines are capable of producing a tremendous amount of energy and have wide industrial applications due to their small size and lower weight. Their efficiency mainly depends on two factors i.e. turbine inlet temperature and compressor and/or turbine efficiency. By increasing the turbine inlet temperature, turbine blades face high-temperature hot corrosion (850 °C to 950 °C) that limits the life of the turbine blade. During hot corrosion, molten sodium salts and vanadium oxide condense over the surface of turbine blades, consume protective oxide layers and diffuse into the microstructure of super alloy. As a result, fatigue and creep phenomena are accelerated leading to fracture. In this paper, the use of hot corrosion-resistant coating i.e. thermal barrier coatings have been investigated. Over the past few years, it has been proven to be an effective strategy to avoid premature failure. Hot corrosion reaction in conventional coatings transforms tetragonal zirconia to monoclinic phase and form large crystalline products which induce thermal stress and cracks upon cooling. While, nanostructured, rare earth elements co-doped and multiple layered thermal barrier coatings possess superior hot corrosion resistance than these conventional coatings. Also, high porosity in nanostructured, low reactivity of rare earth elements, and diffusion hindrance of multilayered coatings resist hot corrosion processes. In conventional metallic bond coatings, hot corrosion destroys protective oxide layers and consumes aluminium and chromium contents. When reinforced with nanoparticles, rare earth elements, and gradient aluminium layers, metallic bond coatings improve their hot corrosion resistance. These modifications develop continuous protective alumina and chromium oxide layer, prohibit diffusion of molten salts, and increase aluminium content of bond coatings. Evaluation of coatings using XRD techniques, SEM spectroscopy, and corrosion kinetics curves exhibit the superiority of hot corrosion-resistant coatings over conventional coatings.

***Keywords*— High-temperature hot corrosion, low-temperature hot corrosion, fatigue life, creep rate, thermal barrier coatings, nanostructured coatings, rare earth elements, gradient coatings**

I. INTRODUCTION

A gas turbine is used to produce a tremendous amount of energy and has many useful applications due to their smaller size and weight. Its efficiency depends mainly on two factors: i.e. higher turbine inlet temperature and efficiency of compressor and turbine. The increase in inlet temperature is driven by improvement in turbine blade metallurgy, coatings, and cooling techniques. Turbine efficiency and blade life are enhanced by hot corrosion, erosion, thermo-mechanical creep, and fatigue properties of turbine blades. Hot corrosion is accelerated due to molten deposits which damages the blade surface [1]. There are two main types of hot corrosion that are discussed in this research work:

A) Type-1: HTHC (high-temperature hot corrosion)

It is observed from 850 to 950°C. The chemical reaction starts due to molten metal on the TBCs (Thermal Barrier Coatings) and sweeps down to substrate material [2, 3]. HTHC is mainly due to Na_2SO_4 (sodium sulfate), NaCl (sodium chloride), and V_2O_4 (Vanadium Oxide). The impurities in fuel can lower the melting point of Na_2SO_4, moreover, during combustion NaCl can form Na_2SO_4 by reacting with SO_2 (sulfur dioxide) and oxygen as shown by the following reaction [4]. Presence of Vanadium accelerates the solubility of turbine blade protective oxide in Na_2SO_4 [5]. It starts by breaking the oxide layer, followed by depletion of chromium content of substrate material, substrate oxidation loss of material integrity which finally leads to blade failure along with material strength.

$$2NaCl\,(l) + SO_2\,(g) + O_2\,(g) \rightarrow Na_2SO_4\,(l) + Cl_2\,(g)$$

B) Type-2: LTHC (low temperature hot corrosion)

It is observed at the temperature range from 650 to 800°C [6]. A high partial pressure SO_3 (sulfur trioxide) formed as a byproduct of combustion leads to LTHC Reaction. The performance of Nano-structured TBCs, rare earth elements, and multilayer TBCs are investigated in this paper. It has been found in recent research that the additions of Nano-structured TBCs, rare earth elements, and multilayer TBCs provide better

performance as compared to the conventional coatings. In this paper, XRD, SEM, and corrosion kinetic curves are used to evaluate different types of coatings.

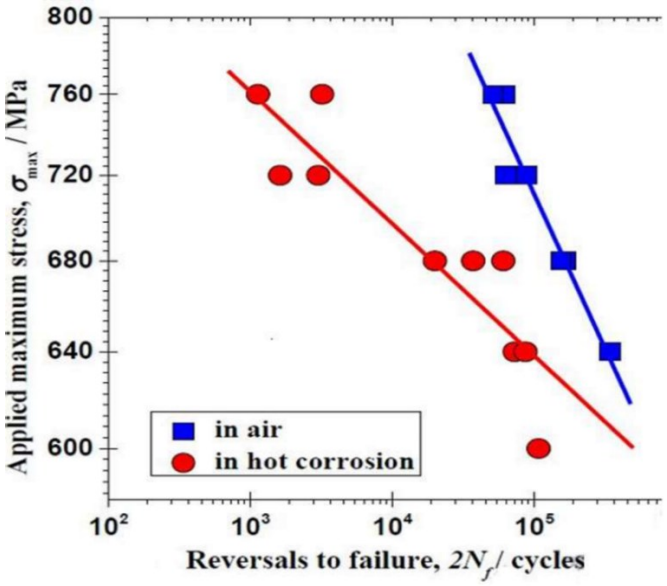

Figure 1 Basquin curve representing the number of cycles to failure for superalloy DZ125 in air and the presence of hot corrosive environment [7].

II. Influence of Hot Corrosion on Turbine Blade Life

With exceptional strength properties at high temperature, Ni (Nickel) based super-alloys are usually used as a substrate material for turbine blades. The mechanical properties of the substrate depending on the chemical composition of refractory elements. Cr (chromium) and Ti (Titanium) are necessary for resistance against hot corrosion [8]. Cr restricts the Na_2SO_4 molten deposits by forming Cr_2O_3 (chromium oxide). Other materials like Nb (Niobium) and Mo (Molybdenum) serves up to 1200 °C and 1300°C, in uncooled systems, respectively. However, hot corrosion challenges the turbine blades and disks as they reduce their fatigue life [9-11]. The fatigue testing of Ni superalloy DZ125 also indicates lower fatigue strength in the presence of a corrosive environment [12]. The Basquin curve presented in Fig. 1 presents a lower fatigue life of DZ125 superalloy in a hot corrosive environment.

Furthermore, hot corrosion experiments done on Ni superalloy 617 has shown that hot corrosion accelerates the creep rate in corrosive environments [13]. During hot corrosion, $M_{23}C_6$ carbides are precipitated at grain boundaries, which depletes Cr and cause inter-granular corrosion. These carbides enhance the fatigue and creep rate of turbine blades due to which, grain boundaries are weakened by the cyclic loadings and lead to fracture. Therefore, to enhance the turbine blade life, resistance against corrosion is essential. Thermal barrier coatings (TBCs) are used as resistance against hot corrosion [14].

III. Hot Corrosion Resistant TBCs

TBCs protect the turbine blade against hot corrosion and thermal stresses, thus enhancing the operating temperature and efficiency of the turbine [15]. They protect turbine blades against thermal shock, hot corrosion, and erosion degradation [16-18]. A TBC consists of a low thermal conductivity topcoat, which protects the substrate against hot corrosion, and the metallic bond coat, which provides adhesion between the topcoat and substrate. The common methods for TBCs applications are EB-PVD (electron beam-physical vapor deposition), HVOFC (high-velocity oxygen fuel coating), and APS (atmospheric plasma spraying) [7, 19, 20]. APS is a widely used deposition because of cost-effectiveness and higher efficiency [21, 22].

Most widely used TBC is Yttria-Stabilized Zirconia (YSZ) [23, 24] However, its performance degrades at the temperature above 1200℃ in the presence of corrosive environment and fuel impurities. These conditions deteriorate TBCs by thermal cycling and spallation by hot corrosion [25-28]. Before the occurrence of hot corrosion reaction, ZrO_2 (Zirconia) is stabilized in the tetragonal phase and stabilized by Y_2O_3 (Yttria) [29, 30]. During hot corrosion, the acidic salts deplete the Y_2O_3 which results in phase transformation of Zirconia from tetragonal to monoclinic phase. This phase transformation leads to additional stresses and cracks in the coatings. Corrosion products induce stresses in TBCs, by reducing their thermal contraction upon cooling [31]. Wide-scale research has been done to improve the effectiveness of TBCs. These research works have focused on Nanostructured TBCs and rare earth metals and compounds.

A) Nanostructured TBCs

Nanostructured YSZ coatings have shown an increase in thermal fatigue, bonding strength, and decreased the thermal conductivity of TBCs in comparison to conventional coatings [32-34]. Hot corrosion experiments of Nanostructured YSZ TBCs have revealed better resistance in the presence of a corrosive environment.

Accelerated corrosion is performed on conventional and nanostructured coating specimens in the presence of 55 wt % V_2O_5 and 45 wt % Na_2SO_4. The specimens are heated at 1000 °C for 30 hours to capture the hot corrosion effects. The

process can be explained by following reactions in the presence of molten salts [35].

$NaVO_3$ formed during the experiments has a low melting point and it easily penetrates the coatings. Where it reacts with Y_2O_3 to transform ZrO_2 from tetragonal to the monoclinic form of YVO_4.

$$ZrO_2.Y_2O_3\ (s) + 2NaVO_3\ (I) \rightarrow m\text{-}ZrO_2\ (l) + 2YVO_4\ (s) + Na_2O\ (I)$$

In addition to the above reaction, V_2O_5 also reacts readily with Y_2O_3 at a temperature above 800 ºC to transform tetragonal Zirconia to monoclinic form.

$$ZrO_2.Y_2O_3\ (s) + V_2O_5\ (I) \rightarrow m\text{-}ZrO_2\ (l) + 2YVO_4\ (s)$$

The stresses and cracking developed by hot corrosion are more pronounced in conventional coatings while nanostructured coatings resist transformation as shown in Fig. 2. High surface roughness and porous zones are formed in nanostructured coatings, which prolong reaction with molten salts and resist ZrO_2 transformation from tetragonal to monoclinic phase. In conventional coatings, cracking starts earlier after 12 hours of exposure to hot corrosion and delamination occurs after 24 hours. However, nanostructured coatings showed resistance to hot corrosion as the development of crack is delayed to 24 hours.

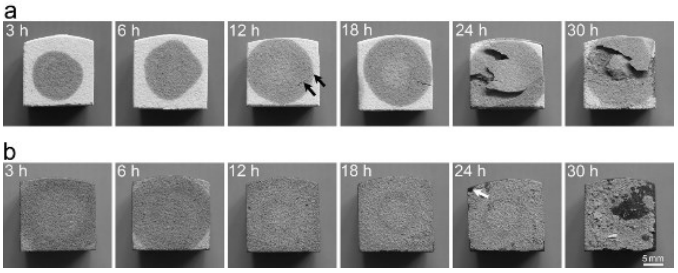

Figure 2 Hot carrion test on Nano-structured and conventional coatings[36].

In recent study, a layer-gradient nanostructured $Sc_2O_3\_Y_2O_3$ co-stabilized Zr_2O_3 (ScYSZ) was compared with convential coatings to improve performance of thermal barrier coatings. The thermal cycling life of ScYSZ is more than that of convential coatings. Also the average insulation temperature of ScYSZ is higher than that of conventional coatings [37].

B) Effect of Rare Earth Elements and Compounds

The addition of rare earth elements or compounds stabilizes YSZ and offers better corrosion resistance than conventional YSZ coatings [38-42]. In experiments, it was found that Scandia and Yttria co-stabilized Zirconia (ScYSZ) offer better corrosion resistance in comparison with Nanostructured YSZ and Scandia [43, 44]. Hot corrosion behavior of ScYSZ is found different from YSZ coatings [45]. In the case of YSZ coatings, spallation occurs in topcoat while in ScYSZ coatings spallation occurs in bond coat [43]. ScYSZ delays the phase transformation of zirconia from tetragonal to monoclinic as shown in X-ray Diffraction (XRD) patterns in Fig.3. Also in ScYSZ, spallation occurs in the bond coat while in YSZ coatings it occurs in the topcoat. Research has shown that Nanostructured Ceria and Yttria co-stabilized Zirconia (CYSZ) exhibits better corrosion resistance than conventional coatings[46]. CeO_2 resists the reaction with the molten salts and obstructs diffusion [47, 48].

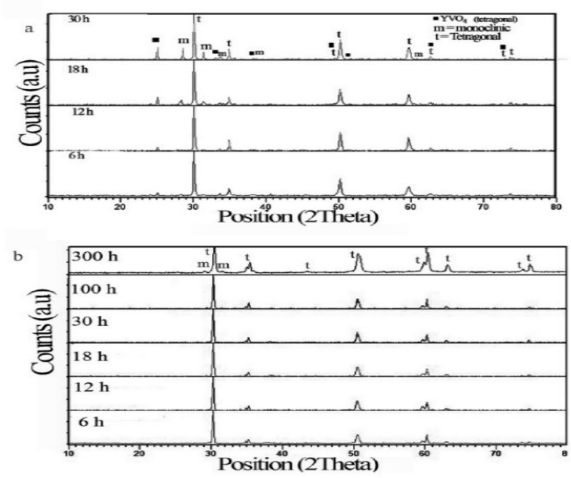

Figure 3 XRD patterns after exposure to hot corrosive environments (a) YSZ (b) ScYSZ [17]

The hot corrosion resistance of Ceria stabilized zirconia (CSZ) coatings is enhanced due to the overlay of alumina (Al_2O_3), as it reduces the infiltration of molten salts and decreases the depletion of Zirconia stabilizers [49]. Higher porosity and lower γ-phase in nano Al_2O_3 resist chemical reaction, which gives it an advantage over micro Al_2O_3. After the hot corrosion test, thermal stresses and cracking occur in CSZ with the transformation of ZrO_2 and formation of irregular shape products of YVO_4, $CeVO_4$, and CeO_3. The extent of degradation in CSZ/ micro Al_2O_3 is lower than CSZ due to the lesser transformation of zirconia. However, no damage and

hot corrosion products are found in layered composite CSZ/nano Al_2O_3 coatings.

It is found in research that corrosion resistance is improved due to less transformation of tetragonal to the monoclinic phase of ZrO_2 in gadolinia (Gd_2O_3), ytterbia (Yb_2O_3) and yttria co-stabilized ZrO_2 (GdYb-YSZ). Yb_2O_3 limits the intensity of GdYb-YSZ to react with molten salts [50]. It acts as a stabilizer for tetragonal ZrO_2 while Y_2O_3 and Gd_2O_3 react with molten salts. After the hot corrosion test, the monoclinic phase content of ZrO_2 in GdYb-YSZ coatings is also less than YSZ coatings. Similarly, $Gd_2Zr_2O_5$ + YSZ and $Gd_2Zr_2O_5$ coatings offer higher corrosion resistance than YSZ coatings, because of less depletion of Y_2O_3. Moreover, development in thermal stresses and cracking in $Gd_2Zr_2O_5$ + YSZ and $Gd_2Zr_2O_5$ coatings takes a longer time in the corrosive environment than YSZ coatings [51].

The hot corrosion test of titania and yttria co-stabilized stabilized zirconia (TiSZ) has revealed the superior performance of TiSZ in comparison with YSZand CSZ [52]. XRD Peaks of coatings obtained after the hot corrosion test indicate no monoclinic phase of ZrO_2 in the case of TiSZ as shown in Fig. 4.

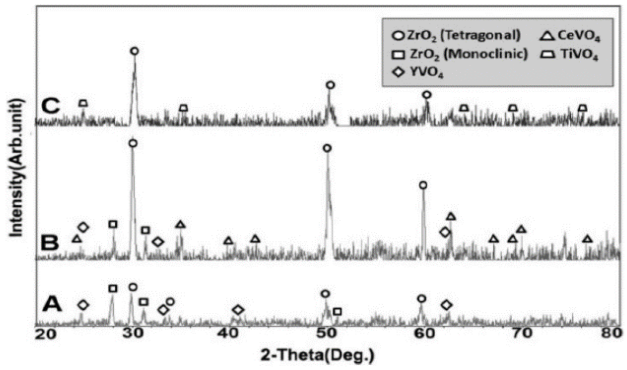

Figure 4 XRD patterns after exposure to hot corrosive environments (a) convention YSZ coatings (b) CSZ coating and (c) TiSZ coatings[52].

Tantalum (Ta) doping on YSZlowers thermal conductivity and stabilizes YSZ up to 1500 °C due to strong interaction between Y^{3+} and Ta^{5+} ions. The hot corrosion resistance of Y_2 O_3 and tantalum oxide (Ta_2O_5) co-doped zirconia coating (TaYSZ) is found superior to YSZ coatings. The reaction of a molten mixture of Na_2SO_4 and V_2O_5 with TaYSZ coatings is weak and reaction products are Na_2TO_3, $TaVO_5$, and Ta_9VO_{25}.

In contrast to YSZ coatings, the TaYSZ coating resist phase transformation and also the corrosion products are very small. Therefore, thermal cracking and stresses in TaYSZ coatings are not induced due to their higher corrosion resistance. The Scanning Electron Microscope (SEM) images of both coatings, developed after the hot corrosion test, are shown in Fig. 5.

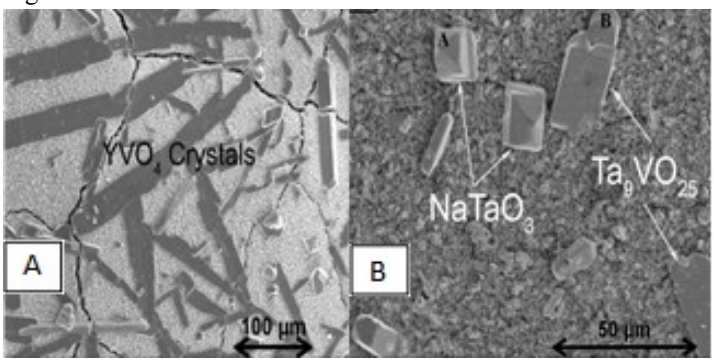

Figure 5 SEM images of (a) conventional YSZ coating and (b) TaYSZ coating developed after hot corrosion tests are presented[53].

C) Hot Corrosion Comparison of Base Metal, Bond Coating, and Multiple Layered TBCs

In one study, the hot corrosion behavior of base metal Inconel 738(BM), NiCrAlY bond coat (BC), duplex YSZ (YSZ/BC), duplex Lanthanum Zirconate (LZ/BC) and a five-layered coated specimen with LZas top layer(LZ+YSZ/YSZ/YSZ+BC)is compared [54]. The hot corrosion resistance of coated specimens is in the following order.

Five Layered coating> YSZ> LZ> BC> BM

The exposure of BM to a molten mixture of Na_2SO_4 and V_2O_5 forms Na_2VO_3 which acts as a catalyst in the oxidation of metallic ions and forms Al_2O_3, Cr_2O_3, NiO . The spinels $NiAl_2O_4$ and $NiCr_2O_4$ formed lead to mass gain, severe strains, and spallation of oxide layers.

The BC provides better corrosion resistance than the BM due to the formation of Al_2O_3 and Cr_2O_3 layers, which prohibits the diffusion of oxidizing agents. The spallation of these oxide layers occurs due to thermal stresses and chemical reaction with molten salts.

Due to hot corrosion in BC, the Al and Ni oxide layers are dissociated because of the fluxing mechanism.

YSZ depicts better hot corrosion resistance than the BC and worse than LZ. However, LZ has low hot corrosion resistance at a higher number of cycles than YSZ, due to propagation of cracks and low fracture toughness. The five-layered coating exhibits better hot corrosion resistance than YSZ and LZ coatings. The top layer reacts with the molten salts and protects the YSZ coatings, Thus it has better corrosion resistance than the YSZ and LZ coatings.

The parabolic corrosion rate constant 'K_p' measures the hot corrosion performance of coatings. Lower 'K_p' indicates better performance of coatings against hot corrosion performance. It is given by the following relation

$$K_p=((\Delta W/A)^2)/t$$

where ΔW/A is the weight gain per unit surface area and 't' is the hot corrosion time.

IV. Hot Corrosion Resistant Metallic Bond Coatings

NiCoCrAlY and NiCrAlYSi coatings are renowned as hot corrosion and oxidation resistant coatings and are also used in bond coats of Thermal Barrier Coatings (TBC) [55]. Al_2O_3 is formed due to the depletion of bond coatings. Al_2O_3layer is a protective layer, but it is not continuous [56]. Thus it causes spallation.

Al_2O_3 reacts with Na_2O to form AlO_2^-, reprecipitating the Al_2O_3 and releasing the O^{2-}. O^{2-} accelerates the formation of Al_2O_3 thus consuming more Al from the coating. In the presence of NaCl, Al_2O_3 is additionally dissolved by the oxychlorination process. To avoid deterioration in mechanical properties, Al content is kept lower than 5 wt %. The application of nanostructured reinforced coatings, doping in rare earth metals and composite/gradient coating is also investigated.

$$Al_2O_3 + 1/2O_2 + NaCl \rightarrow 2NaAlO_2 + Cl_2$$

A) Nanostructured Reinforced Coatings

The addition of nano Al_2O_3, nano SiO_2, and nano CeO_2 exhibits better corrosion resistance in comparison to normal coatings. The mass change of these nano-particle coatings gauges the corrosion performance of such coatings. Mass change is defined as the difference of mass gained from scale formation to mass loss by spallation of oxide scales. Mathematically it is written as

$$M_c = (m_1-m_0 *A_0/A)/ A_1$$

Here M_c is the mass change of coating; m_1, mass change of coated sample; m_0, mass change of uncoated sample; A_0, superficial area of the uncoated part of sample; *A*, superficial area of the uncoated part of sample; A_1, superficial area of the uncoated part of the sample. In the presence of salt (75 w*t* % Na_2SO_4/ 25 *wt* %K_2SO_4) at 1050 °C, the mass change (corrosion kinetics) curves of coatings with and without nanoparticles are shown in Fig. 6.

Fig. 7. Shows that nanoparticle coatings have better corrosion resistance with enhanced thermal fatigue. Whereas, CeO_2 has the best hot corrosion resistance. The addition of nanoparticles serves as the nucleus for heterogeneous nucleation and results in microstructure refinement.

Nanoparticles also enhance corrosion resistance and improve thermal fatigue. Coatings without nanoparticles are affected by spallation and deformation of a surface while no spallation is observed for coatings reinforced by nanoparticles as shown in Fig. 6.

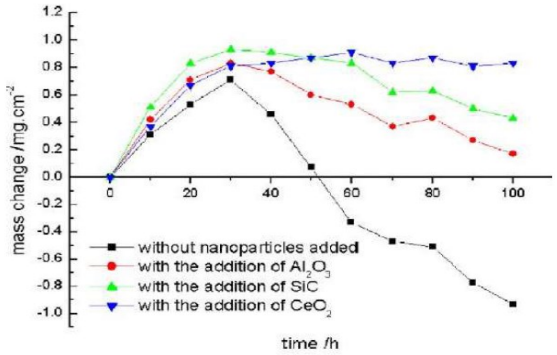

Figure 6 The corrosion kinetics (mass change) curves of NiCoCrAlY coatings [57].

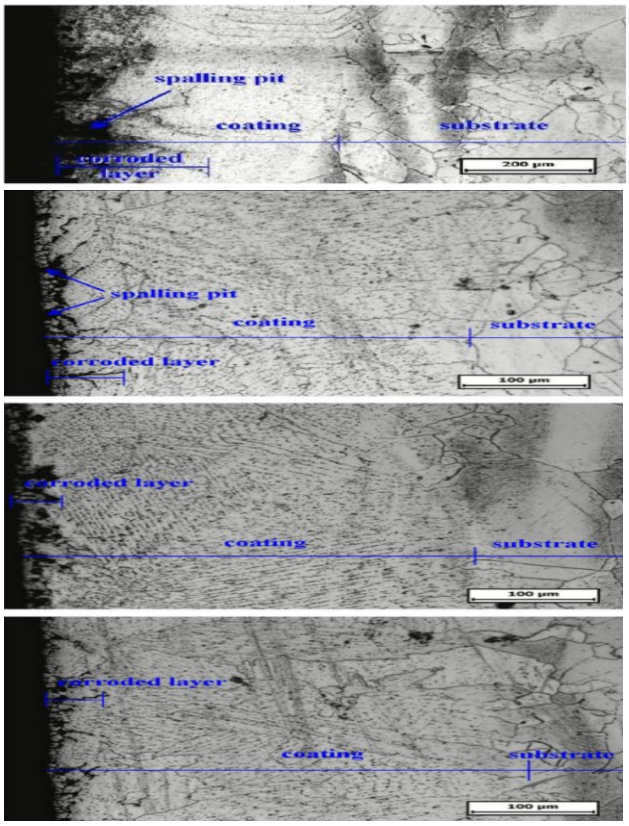

Figure 7 SEM images of (a) NiCoCrAlY coating without nanoparticles, (b) with nano Al2O3, (c) nano SiC and (d) nano CeO2 are displayed [57].

In recent study, APS technique was applied to deposite nano-$Gd_2Zr_2O_7$ (nano-GZ) powder after synthesizing by co-precipitation method on the nickel based substrate. The hot corrosion resistance of conventional coatings was compared with nano-GZ coatings. The hot corrosion resistance of GZ caotings was found found to be more than that of conventional coatings. As nano GZ coatings acts as a barrier to pores and micro-cracks which play a major role in infiltration of molten salts to the TBCs. Fig. 8 shows the XRD patterns of the conventional and nano-GZ coatings [58].

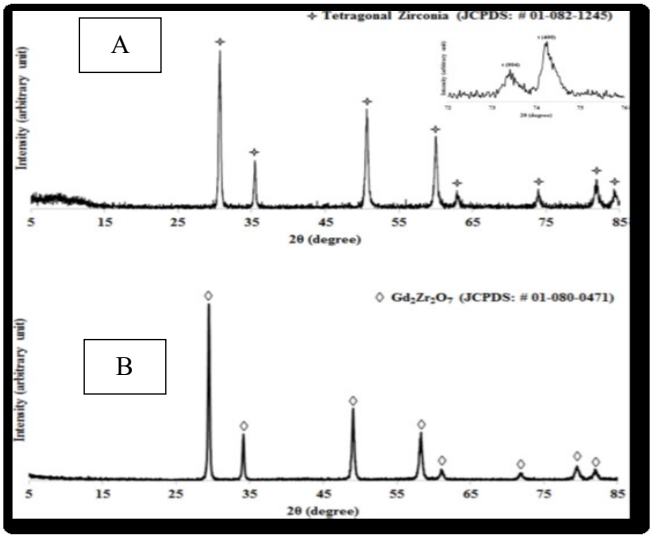

Figure 8 XRD patterns for (A) conventional coatings (B) nano-GZ coatings [58].

B) Doping with Rare Earth Elements

Co-Al-Y-Ce coated specimens have better corrosion resistance and lesser mass gain as compared to Co-Al and Co-Al-Y coated specimens [59]. Co accelerates to the outer layer, and also a synergetic effect is produced to resist hot corrosion due to the doping of Y and Ce [60]. Co enhances the formation of Al_2O_3 in NiAl coatings and lowers the diffusion rate of sulfur [61].

Experiments have also revealed that Co-Al-Si coatings have better corrosion resistance and lower mass gain than the Co-Al coatings [59, 62]. The reason being is the formation of β-NiAl which has higher Al content and it facilitates the formation of Al_2O_3 [63].

$[7]+\gamma'[Ni_3Al] \rightarrow \delta[Ni_2Si] + \beta[NiAl]$

Moreover, SiO_2 is formed as a byproduct, and is resistant to molten salts. Si restricts interdiffusion of an element between coating and substrate. Also, it improves the oxidation resistance of NiAlHf coatings [64].

Pt modified coatings also exhibit better corrosion resistance and lower mass gain due to the transformation of θ- Al_2O_3 to α- Al_2O_3 at initial stages of hot corrosion and formation of Cr_2O_3 which hinders oxygen, sulfur, and chlorine [65].

C) Composite / Gradient NiCoCrAlYSi Coatings

The composite coatings, inner NiCoCrAlYSi layer, and outer AlSiY layer exhibit better corrosion resistance[66]. The gradient NiCoCrAlYSi coatings are prepared by depositing NiCoCrAlYSi target first for 40 microns and then Al target for 10 microns. Normal NiCoCrAlYSi coatings have a thickness of 40 microns. During hot corrosion, Al is consumed rapidly from the normal coating as it offers less resistance to Al diffusion. In composite and gradient coatings more β-NiAl phase is formed which is corrosion resistant. It also serves as an Al reservoir in reaction with corrosive salts thus increasing resistance of composite and gradient coatings. Experiments have shown that gradient coatings have lower mass gain and higher corrosion resistance.

In a recent study, an alloy with chemical composition of Ti-48Al-2Nb-2Cr known as γ-TiAl is employed as substrate. One sample contain one layer and second contains two layers. The experiment was conducted to investigate the microstructure and isothermal oxidation resistance at 1050℃. It was found that due to presence of oxide layers of ZrO2 and Y2O3 a better high isothermal oxidation resistant TBCs are formed. Fig. 8. Shows XRD experimental results of the single and double layered coatings on γ-TiAl substrate [67].

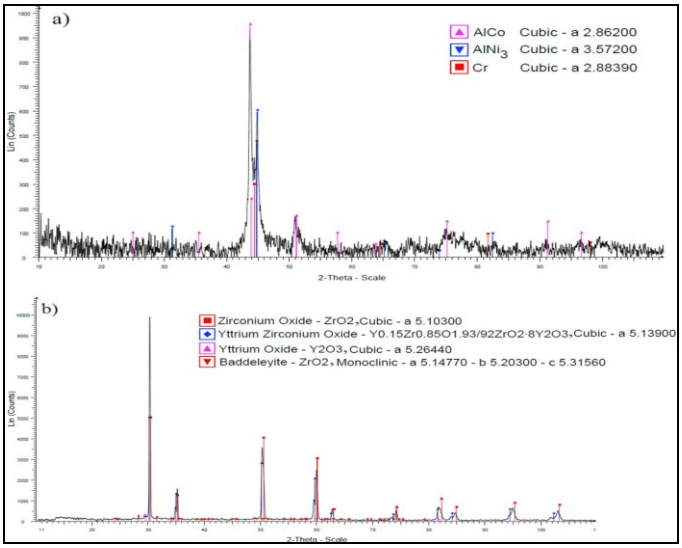

Figure 8 XRD patterns (a) single coating on γ-TiAl (b) double coating on γ-TiAl [67].

V. Conclusion

Hot corrosion occurs at a temperature range of 650 to 950 °C and in the presence of molten sodium salts and vanadium oxide. Resistance against hot corrosion is essential for avoiding premature failures in turbine blades. Nanostructured, rare earth element codoped, and multiple layered thermal barrier coatings have improved hot corrosion resistance. These coatings avoid tetragonal to the monoclinic transformation of zirconia and the formation of large crystalline corrosion products. However, conventional YSZ fails in resisting these two phenomena. Hot corrosion also degrades metallic bond coatings by spallation of protective alumina layer and depletion of aluminium. The addition of nano reinforced particles, rare earth elements, and gradient coatings improve the hot corrosion resistance of metallic bond coats. These additions increase aluminium content, stabilize the protective layer, and prohibit interdiffusion of elements between substrate and coating. XRD, SEM, and corrosion kinetic curves are used to evaluate different types of coatings.

VI. Future Work

Based on the above discussion it is likely that the hot corrosion resistance of turbine blades can be enhanced by the addition of nanoparticles, rare-earth metals, and gradient coatings. However, there is a need to analyze their effects on the properties of coatings, the cost-effectiveness of modifications, and also the comparison of coating techniques like EB-PVD, HVOFC, APS, etc.

VII. Recommendations

A standard hot corrosion testing procedure can be defined as the parameters vary between research works. Fatigue and creep testing of modified coatings may also be done in hot corrosive environments as they are the most affected.

VIII. References

[1] L. Zheng, Z. Maicang, and D. Jianxin, "Hot corrosion behavior of powder metallurgy Rene95 nickel-based superalloy in molten NaCl–Na2SO4 salts," *Materials & Design,* vol. 32, pp. 1981-1989, 2011.

[2] M. Siba, W. Wanmahmood, M. Z. Nuawi, R. Rasani, and M. Nassir, "Flow-induced vibration in pipes: Challenges and solutions—A review," *Journal of Engineering Science and Technology,* vol. 11, pp. 362-382, 2016.

[3] S. Li, X. Yang, and H. Qi, "High-temperature hot-corrosion effects on the creep–fatigue behavior of a directionally solidified nickel-based superalloy: Mechanism and lifetime prediction," *International Journal of Damage Mechanics,* vol. 29, pp. 798-809, 2020.

[4] J. Sahu, B. R. Kumar, S. Das, N. Paulose, and S. Mannan, "Isothermal high temperature low cycle fatigue behavior of Nimonic-263: Influence of type I and type II hot corrosion," *Materials Science and Engineering: A,* vol. 622, pp. 131-138, 2015.

[5] F. Pettit, "Hot corrosion of metals and alloys," *Oxidation of Metals,* vol. 76, pp. 1-21, 2011.

[6] V. Mannava, A. S. Rao, N. Paulose, M. Kamaraj, and R. S. Kottada, "Hot corrosion studies on Ni-base superalloy at 650 C under marine-like environment conditions using three salt mixture (Na2SO4+ NaCl+ NaVO3)," *Corrosion Science,* vol. 105, pp. 109-119, 2016.

[7] R. Steinbrech, V. Postolenko, J. Mönch, J. Malzbender, and L. Singheiser, "Testing method to assess lifetime of EB-PVD thermal barrier coatings on tubular specimens in static and cyclic oxidation tests," *Ceramics International,* vol. 37, pp. 363-368, 2011.

[8] J. Chang, D. Wang, T. Liu, G. Zhang, L. Lou, and J. Zhang, "Role of tantalum in the hot corrosion of a Ni-base single crystal superalloy," *Corrosion Science,* vol. 98, pp. 585-591, 2015.

[9] S. Li, X. Yang, H. Qi, J. Song, and D. Shi, "Low-temperature hot corrosion effects on the low-cycle fatigue lifetime and cracking behaviors of a powder metallurgy Ni-based superalloy," *International Journal of Fatigue,* vol. 116, pp. 334-343, 2018.

[10] P. Jena, R. Singh, L. Mahanta, S. Paswan, and J. Sahu, "Low cycle fatigue behaviour of nickel base superalloy IN 740H at 760° C: Influence of fireside corrosion atmosphere," *International Journal of Fatigue,* vol. 116, pp. 623-633, 2018.

[11] S. Kargarnejad and F. Djavanroodi, "Failure assessment of Nimonic 80A gas turbine blade," *Engineering Failure Analysis,* vol. 26, pp. 211-219, 2012.

[12] X. Yang, S. Li, and H. Qi, "Effect of high-temperature hot corrosion on the low cycle fatigue behavior of a directionally solidified nickel-base superalloy," *International journal of fatigue,* vol. 70, pp. 106-113, 2015.

[13] A. Homaeian and M. Alizadeh, "Interaction of hot corrosion and creep in Alloy 617," *Engineering Failure Analysis,* vol. 66, pp. 373-384, 2016.

[14] R. Synnott, Y. Panchenko, and A. Paczoski, "Turbine blade with hot-corrosion-resistant coating," ed: Google Patents, 2020.

[15] R. Ahmadi-Pidani, R. Shoja-Razavi, R. Mozafarinia, and H. Jamali, "Laser surface modification of plasma sprayed CYSZ thermal barrier coatings," *Ceramics International,* vol. 39, pp. 2473-2480, 2013.

[16] N. P. Padture, "Advanced structural ceramics in aerospace propulsion," *Nature materials,* vol. 15, p. 804, 2016.

[17] C. Ramachandran, V. Balasubramanian, and P. Ananthapadmanabhan, "Thermal cycling behaviour of plasma sprayed lanthanum zirconate based coatings under concurrent infiltration by a molten glass concoction," *Ceramics International,* vol. 39, pp. 1413-1431, 2013.

[18] R. Ahmadi-Pidani, R. Shoja-Razavi, R. Mozafarinia, and H. Jamali, "Improving the thermal shock resistance of plasma sprayed CYSZ thermal barrier coatings by laser surface modification," *Optics and Lasers in Engineering,* vol. 50, pp. 780-786, 2012.

[19] L. Gao, L. Wei, H. Guo, S. Gong, and H. Xu, "Deposition mechanisms of yttria-stabilized zirconia coatings during plasma spray physical vapor deposition," *Ceramics International,* vol. 42, pp. 5530-5536, 2016.

[20] Y. Li, Y. Xie, X. Liu, and X. Zheng, "Effect of physical vapor deposited Al2O3 film on TGO growth in YSZ/CoNiCrAlY coatings," *Ceramics international,* vol. 38, pp. 5113-5121, 2012.

[21] P. R. AHMADI, R. Razavi, R. Mozafarinia, and H. Jamali, "characterization of ceria and yttria stabilized zirconia thermal barrier coatings on in 738 superalloy," 2012.

[22] X. Chen, Y. Zhao, X. Fan, Y. Liu, B. Zou, Y. Wang, H. Ma, and X. Cao, "Thermal cycling failure of new LaMgAl11O19/YSZ double ceramic top coat thermal barrier coating systems,"

Surface and Coatings Technology, vol. 205, pp. 3293-3300, 2011.

[23] S. Bose, *High temperature coatings*: Butterworth-Heinemann, 2017.

[24] C. Roy, M. Noor-A-Alam, A. Choudhuri, and C. Ramana, "Synthesis and microstructure of Gd2O3-doped HfO2 ceramics," *Ceramics International,* vol. 38, pp. 1801-1806, 2012.

[25] L. Guo, M. Li, and F. Ye, "Comparison of hot corrosion resistance of Sm2Zr2O7 and (Sm0. 5Sc0. 5) 2Zr2O7 ceramics in Na2SO4+ V2O5 molten salt," *Ceramics International,* vol. 42, pp. 13849-13854, 2016.

[26] I. N. Qureshi, M. Shahid, and A. N. Khan, "Hot corrosion of yttria-stabilized zirconia coating, in a mixture of sodium sulfate and vanadium oxide at 950 C," *Journal of Thermal Spray Technology,* vol. 25, pp. 567-579, 2016.

[27] L. Gao, H. Guo, L. Wei, C. Li, S. Gong, and H. Xu, "Microstructure and mechanical properties of yttria stabilized zirconia coatings prepared by plasma spray physical vapor deposition," *Ceramics International,* vol. 41, pp. 8305-8311, 2015.

[28] Y. Yin, W. Ma, X. Jin, X. Li, Y. Bai, R. Jia, and H. Dong, "Hot corrosion behavior of the La2 (Zr0. 7Ce0. 3) 2O7 ceramic in molten V2O5 and a Na2SO4+ V2O5 salt mixture," *Journal of Alloys and Compounds,* vol. 689, pp. 123-129, 2016.

[29] Y. Hui, S. Zhao, J. Xu, B. Zou, Y. Wang, X. Cai, L. Zhu, and X. Cao, "High-temperature corrosion behavior of zirconia ceramic in molten Na2SO4+ NaVO3 salt mixture," *Ceramics International,* vol. 42, pp. 341-350, 2016.

[30] H. Huang, C. Liu, L. Ni, and C. Zhou, "Evaluation of microstructural evolution of thermal barrier coatings exposed to Na2SO4 using impedance spectroscopy," *Corrosion Science,* vol. 53, pp. 1369-1374, 2011.

[31] M. Saremi and M. Habibi, "An Investigation on Hot Corrosion Resistance of Plasma Sprayed YSZ - Ceria TBC in Na2SO4+ V2O5 at 1050 ° C," *Supplemental Proceedings: Materials Processing and Energy Materials,* vol. 1, pp. 429-437, 2011.

[32] A. Keyvani, M. Saremi, M. H. Sohi, Z. Valefi, M. Yeganeh, and A. Kobayashi, "Microstructural stability of nanostructured YSZ–alumina composite TBC compared to conventional YSZ coatings by means of oxidation and hot corrosion tests," *Journal of alloys and compounds,* vol. 600, pp. 151-158, 2014.

[33] H. Jamali, R. Mozafarinia, R. Shoja Razavi, R. Ahmadi-Pidani, and M. Reza Loghman-Estarki, "Fabrication and evaluation of plasma-sprayed nanostructured and conventional YSZ thermal barrier coatings," *Current nanoscience,* vol. 8, pp. 402-409, 2012.

[34] H. Jamali, R. Mozafarinia, R. S. Razavi, and R. Ahmadi-Pidani, "Comparison of thermal shock resistances of plasma-sprayed nanostructured and conventional yttria stabilized zirconia thermal barrier coatings," *Ceramics International,* vol. 38, pp. 6705-6712, 2012.

[35] S. Yugeswaran, A. Kobayashi, and P. Ananthapadmanabhan, "Initial phase hot corrosion mechanism of gas tunnel type plasma sprayed thermal barrier coatings," *Materials Science and Engineering: B,* vol. 177, pp. 536-542, 2012.

[36] H. Jamali, R. Mozafarinia, R. Shoja-Razavi, and R. Ahmadi-Pidani, "Comparison of hot corrosion behaviors of plasma-sprayed nanostructured and conventional YSZ thermal barrier coatings exposure to molten vanadium pentoxide and sodium sulfate," *Journal of the European Ceramic Society,* vol. 34, pp. 485-492, 2014.

[37] W. Fan, Y. Bai, Y. Wang, T. He, Y. Gao, Y. Zhang, X. Zhong, B. Li, Z. Chang, and Y. Ma, "Microstructural design and thermal cycling performance of a novel layer-gradient nanostructured Sc2O3–Y2O3 co-stabilized ZrO2 thermal barrier coating," *Journal of Alloys and Compounds,* p. 154525, 2020.

[38] L. Guo, M. Li, C. Yang, C. Zhang, L. Xu, F. Ye, C. Dan, and V. Ji, "Calcium-magnesium-alumina-silicate (CMAS) resistance property of BaLn2Ti3O10 (Ln= La, Nd) for thermal barrier coating applications," *Ceramics International,* vol. 43, pp. 10521-10527, 2017.

[39] F. Wang, L. Guo, C. Wang, and F. Ye, "Calcium-magnesium-alumina-silicate (CMAS) resistance characteristics of LnPO4 (Ln= Nd, Sm, Gd) thermal barrier oxides," *Journal of the European Ceramic Society,* vol. 37, pp. 289-296, 2017.

[40] X. Xiaoyun, G. Hongbo, G. Shengkai, and X. Huibin, "Hot corrosion behavior of double-ceramic-layer LaTi2Al9O19/YSZ thermal barrier coatings," *Chinese Journal of Aeronautics,* vol. 25, pp. 137-142, 2012.

[41] A. Bhattachaya, V. Shklover, K. Kunze, and W. Steurer, "Effect of 7YSZ on the long-term stability of YTaO4 doped ZrO2 system," *Journal of the European Ceramic Society,* vol. 31, pp. 2897-2901, 2011.

[42] S. Li, Z.-G. Liu, and J.-H. Ouyang, "Study on hot corrosion reactions between SmYbZr2O7 ceramic and vanadium pentoxide at temperatures of 600–1000° C in air," *Materials Chemistry and Physics,* vol. 130, pp. 1134-1138, 2011.

[43] M. Loghman-Estarki, R. S. Razavi, H. Edris, S. Bakhshi, M. Nejati, and H. Jamali, "Comparison of hot corrosion behavior of nanostructured ScYSZ and YSZ thermal barrier coatings," *Ceramics international,* vol. 42, pp. 7432-7439, 2016.

[44] H.-f. Liu, X. Xiong, X.-b. Li, and Y.-l. Wang, "Hot corrosion behavior of Sc2O3–Y2O3–ZrO2 thermal barrier coatings in presence of Na2SO4+ V2O5 molten salt," *Corrosion science,* vol. 85, pp. 87-93, 2014.

[45] M. R. Loghman-Estarki, M. Nejati, H. Edris, R. S. Razavi, H. Jamali, and A. H. Pakseresht, "Evaluation of hot corrosion behavior of plasma sprayed scandia and yttria co-stabilized nanostructured thermal barrier coatings in the presence of molten sulfate and vanadate salt," *Journal of the European Ceramic Society,* vol. 35, pp. 693-702, 2015.

[46] M. Hajizadeh-Oghaz, R. S. Razavi, A. Ghasemi, and Z. Valefi, "Na2SO4 and V2O5 molten salts corrosion resistance of plasma-sprayed nanostructured ceria and yttria co-stabilized zirconia thermal barrier coatings," *Ceramics International,* vol. 42, pp. 5433-5446, 2016.

[47] J. Kärger, D. M. Ruthven, and D. N. Theodorou, *Diffusion in nanoporous materials*: John Wiley & Sons, 2012.

[48] M. Saremi, A. Keyvani, and M. Heydarzadeh Sohi, "Hot corrosion resistance and mechanical behavior of atmospheric plasma sprayed conventional and nanostructured zirconia coatings," in *International Journal of Modern Physics: Conference Series*, 2012, pp. 720-727.

[49] M. Nejati, M. Rahimipour, and I. Mobasherpour, "Evaluation of hot corrosion behavior of CSZ, CSZ/micro Al2O3 and CSZ/nano Al2O3 plasma sprayed thermal barrier coatings," *Ceramics International,* vol. 40, pp. 4579-4590, 2014.

[50] L. Guo, C. Zhang, M. Li, W. Sun, Z. Zhang, and F. Ye, "Hot corrosion evaluation of Gd2O3-Yb2O3 co-doped Y2O3 stabilized ZrO2 thermal barrier oxides exposed to Na2SO4+ V2O5 molten salt," *Ceramics International,* vol. 43, pp. 2780-2785, 2017.

[51] M. Habibi, L. Wang, and S. Guo, "Evolution of hot corrosion resistance of YSZ, Gd2Zr2O7, and Gd2Zr2O7+ YSZ composite thermal barrier coatings in Na2SO4+ V2O5 at 1050° C," *Journal of the European Ceramic Society,* vol. 32, pp. 1635-1642, 2012.

[52] M. Habibi and S. Guo, "The hot corrosion behavior of plasma sprayed zirconia coatings stabilized with yttria, ceria, and titania in sodium sulfate and vanadium oxide," *Materials and Corrosion,* vol. 66, pp. 270-277, 2015.

[53] M. Habibi, L. Wang, J. Liang, and S. Guo, "An investigation on hot corrosion behavior of YSZ-Ta2O5 in Na2SO4+ V2O5 salt at 1100° C," *Corrosion science,* vol. 75, pp. 409-414, 2013.

[54] C. Ramachandran, V. Balasubramanian, and P. Ananthapadmanabhan, "On the cyclic hot corrosion behaviour of atmospheric plasma sprayed Lanthanum Zirconate based coatings in contact with a mixture of sodium sulphate and vanadate salts: A comparison with the traditional Ysz duplex and NiCrAlY coated samples," *Vacuum,* vol. 97, pp. 81-95, 2013.

[55] L. Shi, L. Xin, X. Wang, X. Wang, H. Wei, S. Zhu, and F. Wang, "Influences of MCrAlY coatings on oxidation resistance

of single crystal superalloy DD98M and their inter-diffusion behaviors," *Journal of Alloys and Compounds,* vol. 649, pp. 515-530, 2015.

[56] K. Zhang, M. Liu, S. Liu, C. Sun, and F. Wang, "Hot corrosion behaviour of a cobalt-base super-alloy K40S with and without NiCrAlYSi coating," *Corrosion Science,* vol. 53, pp. 1990-1998, 2011.

[57] H. Wang, D. Zuo, G. Chen, G. Sun, X. Li, and X. Cheng, "Hot corrosion behaviour of low Al NiCoCrAlY cladded coatings reinforced by nano-particles on a Ni-base super alloy," *Corrosion Science,* vol. 52, pp. 3561-3567, 2010.

[58] M. Bahamirian, S. Hadavi, M. Farvizi, M. Rahimipour, and A. Keyvani, "Enhancement of hot corrosion resistance of thermal barrier coatings by using nanostructured Gd2Zr2O7 coating," *Surface and Coatings Technology,* vol. 360, pp. 1-12, 2019.

[59] Z. Liu, X. Zhao, and C. Zhou, "Improved hot corrosion resistance of Y–Ce–Co-modified aluminide coating on nickel base superalloys by pack cementation process," *Corrosion Science,* vol. 92, pp. 148-154, 2015.

[60] H. Guo, D. Li, L. Zheng, S. Gong, and H. Xu, "Effect of co-doping of two reactive elements on alumina scale growth of β-NiAl at 1200° C," *Corrosion science,* vol. 88, pp. 197-208, 2014.

[61] Q. Fan, S. Jiang, H. Yu, J. Gong, and C. Sun, "Microstructure and hot corrosion behaviors of two Co modified aluminide coatings on a Ni-based superalloy at 700 C," *Applied surface science,* vol. 311, pp. 214-223, 2014.

[62] H. He, Z. Liu, W. Wang, and C. Zhou, "Microstructure and hot corrosion behavior of Co–Si modified aluminide coating on nickel based superalloys," *Corrosion Science,* vol. 100, pp. 466-473, 2015.

[63] C. Fu, W. Kong, and G. Cao, "Microstructure and oxidation behavior of Al+ Si co-deposited coatings on nickel-based superalloys," *Surface and Coatings Technology,* vol. 258, pp. 347-352, 2014.

[64] P. Dai, Q. Wu, Y. Ma, S. Li, and S. Gong, "The effect of silicon on the oxidation behavior of NiAlHf coating system," *Applied surface science,* vol. 271, pp. 311-316, 2013.

[65] R. Liu, S. Jiang, H. Yu, J. Gong, and C. Sun, "Preparation and hot corrosion behaviour of Pt modified AlSiY coating on a Ni-based superalloy," *Corrosion Science,* vol. 104, pp. 162-172, 2016.

[66] J. Ma, S. M. Jiang, J. Gong, and C. Sun, "Hot corrosion properties of composite coatings in the presence of NaCl at 700 and 900° C," *Corrosion science,* vol. 70, pp. 29-36, 2013.

[67] S. Nouri, S. Sahmani, M. Asayesh, and M. M. Aghdam, "Microstructural characterization of YSZ-CoNiCrAlY two-layered thermal barrier coating formed on γ-TiAl intermetallic alloy via APS process," *Intermetallics,* vol. 118, p. 106704, 2020.